A visible-light-induced photoelectrochemical water-splitting system featuring an organo-photocathode along with a tungsten oxide photoanode†

Yuto Kawai,[a] Keiji Nagai[b] and Toshiyuki Abe (iD) *[a]

A photoelectrochemical water-splitting system featuring an organo-photocathode of a p–n bilayer was studied, where WO_3 was simultaneously utilized as a photoanode. Stoichiometric formation of H_2 and O_2 was found to occur due to the decomposition of water. In the reference system of a WO_3 photoanode and Pt counter electrode, bias voltages more than 0.4 V were needed to be applied for water splitting; however, the present system successfully led to water decomposition by applying only a low voltage of 0.1 V to the system. In the present water-splitting system, oxidizing and reducing powers can be separately generated at the WO_3 photoanode and organo-photocathode, respectively, which is distinct from the reference system. Furthermore, electron transfer from WO_3 (conduction band) to the hole-retained p-type layer (valence band) in the organo-photocathode can efficiently occur for completing the photoelectrochemical process, thus, resulting in a high concentration of holes available for rate-limiting O_2 evolution at WO_3 on the basis of efficient charge separation.

Introduction

Solar hydrogen has attracted attention as a potential clean energy for establishing a sustainable society. The most ideal and ultimate method for acquiring solar hydrogen is water photolysis. Hence, the photoelectrochemical and photocatalytic decomposition of water has been actively investigated.[1–10] The construction of an efficient water-splitting system under solar irradiation is the most central issue. Tungsten(VI) oxide (WO_3) is a photocatalyst material capable of water oxidation to O_2; here, the metal oxide has been realized as a photoanode for O_2 evolution.[10–17] WO_3 cannot solely lead to the overall decomposition of water because the reducing power generated at its conduction band edge is insufficient for the evolution of H_2 from H^+.[18–21] In other words, some of the metal oxides (such as WO_3, Fe_2O_3, *etc.*) can respond to visible-light energy; however, their conduction band edge of the d-orbital is forced on a downward shift, making it impossible for the reduction of

H^+.[18–21] With respect to the position of valence band edge corresponding to oxidizing power, WO_3 is similar to TiO_2.[20–23] Therefore, making an effective use of the oxidizing power of WO_3 can help in developing a visible-light-induced water-splitting system. For instance, when employing a system featuring an organo-photocathode for photoelectrochemical water splitting (*cf.* Scheme 1), TiO_2 photoanode was utilized in the overall splitting of water, particularly under bias-free condition.[4] As reported by Honda and Fujishima,[24] the water-splitting system, comprising TiO_2 photoanode and Pt counter, is a typical instance, but it required chemical or electric bias for completing the water splitting process.[25–29]

[a]Department of Frontier Materials Chemistry, Graduate School of Science and Technology, Hirosaki University, 3 Bunkyo-cho, Hirosaki 036-8561, Japan. E-mail: tabe@hirosaki-u.ac.jp

[b]Laboratory for Chemistry and Life Science, Institute of Innovative Research, Tokyo Institute of Technology, Suzukake-dai, Midori-ku, Yokohama 226-8503, Japan

† Electronic supplementary information (ESI) available: Experimental details, cyclic voltammograms at photoelectrodes, action spectrum for photocurrents generated at WO_3, and its absorption spectrum and SEM images, and data of photoelectrochemical water splitting in the reference WO_3–Pt system. See DOI: 10.1039/c7ra05272c

Scheme 1 An illustration of the system employed for water splitting.

This journal is © The Royal Society of Chemistry 2017

Photoelectrochemical and photocatalytic systems based on the utilization of both organic semiconductors and p–n bilayer have been studied by our group.[30–40] For example, an organic p–n bilayer of phthalocyanine [MPc (M = H_2 or Zn), p-type] and fullerene (C_{60}, n-type) can function as a photocathode, where a reducing power can be generated at the C_{60}/water interface through a series of photophysical events within the bilayer.[38–40] Particularly, in terms of molecular hydrogen evolution, when loading Pt on the C_{60} surface in the MPc/C_{60} organo-photocathode, it induced the reduction of H^+ at applied potentials that are more positive than the formal potential of H^+/H_2.[39,40]

In the present study, a photoelectrochemical water-splitting system was investigated, where WO_3 (photoanode) and Pt-loaded ZnPc/C_{60} bilayer (photocathode, *vide supra*) were simultaneously employed in the system depicted in Scheme 1. The stoichiometric decomposition of water into H_2 and O_2 occurred on applying a bias voltage less than the theoretical voltage of 1.23 V. It is noted that the present system successfully led to water decomposition under a low bias condition (*i.e.* 0.1 V), where a reference system of WO_3 photoanode and Pt counter cannot induce the redox reaction of water. Details of the results are discussed in the following sections.

Experimental

The ZnPc/C_{60} bilayer was prepared by vapor deposition (pressure, <1.0×10^{-3} Pa; deposition speed, *ca.* 0.03 nm s^{-1}) using an indium-tin-oxide (ITO)-coated glass plate as the base material.[40] ZnPc was first coated on ITO, followed by the coating of C_{60} on top of the ZnPc layer; moreover, a Pt co-catalyst was photocathodically deposited onto the C_{60} surface of the bilayer.[39,40] The resulting photocathode is abbreviated as ITO/ZnPc/C_{60}–Pt. A WO_3 film coated on an F-doped tin oxide (FTO) was prepared according to the following procedures. WO_3 (72 g, Kojundo Chemical Laboratory) and acetylacetone (0.8 mL, Wako Chemical) were mixed well in a mortar, and then, pure water (24 mL) was slowly added during 2 h. Subsequently, Triton X-100 detergent (1 mL, Aldrich) was added and mixed well with the resulting slurry of WO_3, following which the mixture was subject to ultrasonic irradiation. Furthermore, the sample was centrifuged to eliminate large-sized particles of WO_3 (1000 rpm, 5 min). This centrifugation process was repeated 3 times. The resulting suspension of WO_3 (800 μL) was spin-coated (2000 rpm, 1 min) on an FTO electrode (4 × 4 cm), followed by drying at 373 K for 30 min. The processes of both spin-coating and drying were repeated 3 times. Prior to use, the resulting film was calcined in an electric furnace [at 823 K for 2 h (rate of temperature rising: 2 °C min^{-1})]. The SEM image of the WO_3 film is shown in Fig. S1 (in the ESI†). The photoanode of WO_3 is denoted as FTO/WO_3. FTO is usually utilized in preparing photoelectrodes at a high temperature, in order to avoid an unfavorable increase of sheet resistance.[41] The preparation of FTO/WO_3 was conducted by modifying a method for FTO/TiO_2.[41] The aforementioned conditions of FTO/WO_3 preparation were optimal (*cf.* thickness of WO_3, *ca.* 1 μm). The effective area of all the photoelectrodes employed was 1 cm ×

1 cm. A cell made up of twin compartments separated by a salt bridge was utilized for the water-splitting studies (see Scheme 1). All studies were performed under an Ar atmosphere in an aqueous H_3PO_4 solution (pH = 2). Other experimental details are provided in the ESI.†

Results and discussion

Cyclic voltammogram (CV) was measured at FTO/WO_3 photoanode in an H_3PO_4 solution (Fig. S2 in the ESI†), where a three-electrode system was employed for the voltammetric measurement (see Scheme S1 in the ESI†). CV measured at ITO/ZnPc/C_{60}–Pt photocathode is also depicted in Fig. S2.†[40] Considering the formal potentials for H^+ reduction (−0.32 V *vs.* Ag/AgCl (sat.) for H^+/H_2 couple) and water oxidation (+0.91 V *vs.* Ag/AgCl (sat.) for O_2/H_2O couple) at pH = 2, the voltammograms indicated that the photo-induced reactions for H_2 evolution and O_2 evolution can efficiently occur at both photoelectrodes. In other words, a photoelectrochemical water splitting can be expected to take place under the condition of a low bias voltage, on the basis of the evidence that both photoanodic and photocathodic currents occurred at close potentials.

In addition, action spectrum for the photocurrents generated at FTO/WO_3 photoanode was measured, where the same setup as the voltammetric measurement was employed (*cf.* Scheme S1†). The resulting action spectrum acquired at the photoanode of WO_3 was consistent with its absorption spectrum (Fig. S1†), indicating that a photocurrent can be generated due to the band-gap excitation of WO_3 [*cf.* the magnitude of its band-gap was in accordance with the reported value (*ca.* 2.7 eV) corresponding to the absorption edge of *ca.* 460 nm[18,21,23,42,43]]. As for the ITO/ZnPc/C_{60}–Pt photocathode capable of H_2 evolution, its action spectrum has previously been clarified to originate in the entire visible-light absorption of both ZnPc and C_{60}.[40]

According to Scheme 1, a photoelectrochemical water splitting was studied by applying bias voltages to the system. As a result, H_2 evolution was found to occur along with O_2 evolution, particularly at bias voltages less than 1.23 V (the theoretical voltage for water splitting). In other words, the stoichiometric decomposition of water took place in the present system. Fig. 1 shows the relationships between the amounts of H_2 and O_2 evolved and the applied voltages. Note that the application of only a low bias voltage of 0.1 V to the system led to water splitting, although voltages more than 0.3 V are usually needed to be applied to the reference system of WO_3 photoanode and Pt counter (*vide infra*).[11,15–17,21,44,45] The H_2 and O_2 amounts essentially increased with elevating applied voltages; however, the evolved amounts became gentle at voltages larger than 0.6 V. Based on the data of water splitting, the light-to-hydrogen conversion efficiency (η, see the ESI† concerning the calculation method) was estimated with respect to the applied voltages (Fig. 1). The most efficient water splitting occurred at 0.6 V with *ca.* 0.07% while the η value decreased with higher voltages. Applied bias voltages can lead to efficient charge separation along with an efficient charge transfer between both photoelectrodes, where the amounts of H_2 and O_2 may increase to involve the increasing concentration of carriers available for
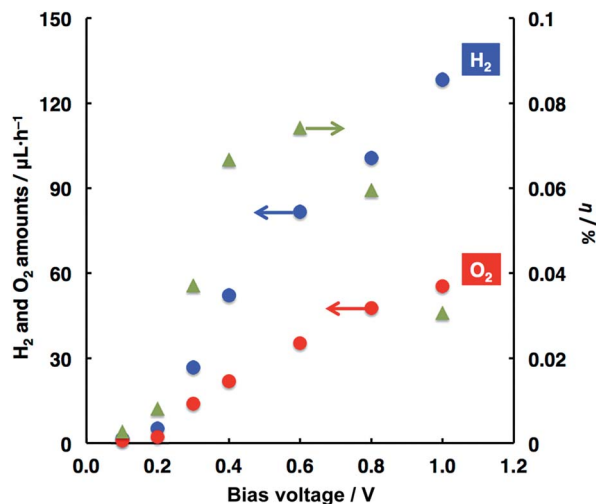
Fig. 1 Relationships of the evolved H_2 and O_2 amounts and η values with applied voltages. This study was conducted in the two-electrode system depicted in Scheme 1. Faradaic efficiencies for H_2 and O_2 evolution were typically >90% and >80%, respectively (see ESI†). Photoanode, WO_3 (geometrical area, 1 cm²); photocathode, ITO/ZnPc (75 nm)/C_{60} (125 nm)–Pt (geometrical area, 1 cm²); electrolyte, H_3PO_4 solution (pH = 2); light intensity (for photoanode), *ca.* 50 mW cm⁻²; light intensity (for photocathode), *ca.* 90 mW cm⁻².

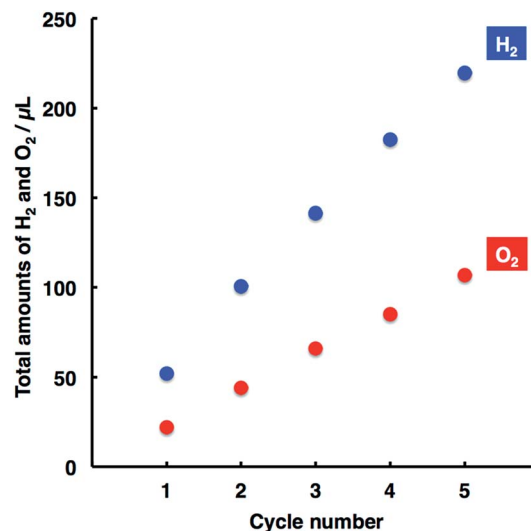**Fig. 2** Relationships between the H_2 and O_2 amounts with cycle number. Experimental conditions were the same as those used in Fig. 1. The bias voltage of 0.4 V was applied to the system, and the irradiation time was 1 h per one cycle.

water decomposition. A decreasing value of η is attributed to a non-linear increase of carrier concentration with applied voltages, thus resulting in a moderate enhancement of kinetics for H_2 and O_2 formation. Such a phenomenon was also represented in another system of photoelectrochemical water splitting.[4,44–49]

A prolonged study of water splitting was conducted to examine the durability of the present system, where both photoanode and photocathode were repeatedly used with the cycle number. As shown in Fig. 2, the amounts of H_2 and O_2 evolved linearly increased with the cycle number, demonstrating stable and durable performance for water splitting.

Control experiments were conducted in the presence of methanol (electron donor) or Fe^{3+} ion (electron acceptor), which are compared with a typical result of photoelectrochemical water splitting (Table 1). Irrespective of the presence of Fe^{3+} ion, the amount of O_2 evolved was almost constant (Entries 1 and 2). The evolved amount of H_2 noticeably increased in the presence of methanol (Entry 3). Therefore, these results suggest that the present system (*i.e.* Entry 1) is kinetically dominated by the evolution of O_2 from water.

A reference system of WO_3 photoanode and Pt counter (denoted as WO_3–Pt system) was examined for photoelectrochemical water splitting. The results are summarized in Fig. S3.† The WO_3–Pt system resulted in the evolution of both H_2 and O_2 only when high voltages (*i.e.* ≥0.4 V) were applied to the system. This is reasonable since the bottom edge of the conduction band of WO_3, corresponding to the position of reducing power, is 0.3 V positive for the formal potential of H^+/H_2 (*vide supra*).[18–21] Fig. S3† showed similar dependencies of both the evolved amounts and η values on bias voltages to Fig. 1. In a separate experiment, the rate-limiting reaction in the WO_3–Pt

system was investigated in the presence of methanol or Fe^{3+} ion. As shown in Table S1 (in the ESI†), it was confirmed that the rate-limiting O_2 evolution occurs in the reference system.

As for WO_3 photoanode[10–17] and ITO/ZnPc/C_{60}–Pt photocathode,[40] those photoelectrochemical reactivities for water reaction have previously been elucidated. The most typical characteristics of the present system are that oxidizing and reducing powers are separately generated at WO_3 and ITO/ZnPc/C_{60}–Pt, respectively. Furthermore, as indicated in Scheme 1, the excited electron generated at WO_3 can be transferred to the hole-remained valence band of ZnPc for accomplishing photoelectrochemical water splitting, through which the pristine species of WO_3 and ZnPc can be regenerated. This is distinct from the reference WO_3–Pt system where the reducing power photogenerated at WO_3 can directly participate in the evolution of H_2 from H^+. In Table 2, the typical comparison of the WO_3–Pt system with the WO_3 and ITO/ZnPc/C_{60}–Pt system is shown. As aforementioned, those systems involve the rate-limiting O_2 evolution. The amounts of H_2 and O_2 originating from water

Table 1 Control experiment data with the WO_3 (photoanode) and ITO/ZnPc/C_{60}–Pt (photocathode) system[a]

System	H_2 amount ($\mu L\ h^{-1}$)	O_2 amount ($\mu L\ h^{-1}$)	Note
Entry 1[b]	81.8	35.4	No control system
Entry 2[c]	150	—	In the presence of methanol
Entry 3[d]	—	34.0	In the presence of Fe^{3+}

[a] Bias voltage of 0.6 V was applied for the system with experimental conditions similar to those in Fig. 1. [b] Data from Fig. 1. [c] A methanol solution (methanol/water(v/v) = 1 : 1, pH = 2) was used. [d] An aqueous solution of $Fe(NO_3)_3$ (5 mM, pH = 2) was employed.

Table 2 Comparison of water splitting data in the present system to the WO_3–Pt system[a]

System	Photoanode	Cathode	H_2 amount ($\mu L\ h^{-1}$)	O_2 amount ($\mu L\ h^{-1}$)
Entry 1[b]	WO_3	$ITO/ZnPc/C_{60}$–Pt	81.8	35.4
Entry 2[c]	WO_3	Pt wire	13.5	7.82

[a] Bias voltage of 0.6 V was applied to the system, and other experimental conditions were similar to those of Fig. 1. [b] Data from Fig. 1. [c] Instead of $ITO/ZnPc/C_{60}$–Pt, a Pt wire was employed as a cathode; data listed in this table can also be seen in Fig. S3.†

splitting were greater in the latter system. The difference between those systems is attributable to the magnitude of charge separation. In other words, the steady concentration of holes available for O_2 evolution can be considered to be higher in the WO_3 and $ITO/ZnPc/C_{60}$–Pt system. This may indicate that the electron transport between the photoelectrodes employed (*vide supra*) efficiently occurs for producing the higher concentration of carriers.

Conclusions

This work studied the photoelectrochemical water-splitting system featuring an organo-photocathode along with a WO_3 photoanode, where the stoichiometric decomposition of water into H_2 and O_2 was found to occur. Based on the action spectral characteristics of both $ITO/ZnPc/C_{60}$–Pt photocathode and WO_3 photoanode, a visible-light energy was available for water splitting. In the reference WO_3–Pt system, the bias voltages more than 0.4 V needed to be applied for evolving H_2 and O_2; however, the present system demonstrated that extremely low-biased water splitting can occur. Distinct from the reference system, oxidizing and reducing powers for water splitting were separately generated at WO_3 photoanode and $ITO/ZnPc/C_{60}$–Pt photocathode, respectively. Irrespective of the systems studied, the evolution of O_2 from water was the rate-limiting step. However, in the present system, the electron transfer from WO_3 (CB) to hole-remained ZnPc (VB) can efficiently occur for producing a high concentration of carriers available for O_2 evolution. The application of two types of materials for water splitting is an effective method, which can be seen in the Z-scheme type photocatalytic water-splitting system[50–52] as well as the present system. In these systems, the materials, which cannot solely participate in the overall decomposition of water, can play active parts. The utilization of distinct types of materials may also have merits in terms of harvesting of solar energy. Photoelectrochemical water decomposition is one of the most promising approaches for acquiring solar hydrogen. In this context, developing efficient photoelectrodes is a vital issue for establishing a practical water-splitting system.

Acknowledgements

References

1 J. Su, L. Zhu and G. Chen, *Appl. Catal., B*, 2016, **186**, 127–135.
2 M. Kodera, H. Urabe, M. Katayama, T. Hisatomi, T. Minegishi and K. Domen, *J. Mater. Chem. A*, 2016, **4**, 7658–7664.
3 S. Ida, K. Yamada, M. Matsuka, H. Hagiwara and T. Ishihara, *Electrochim. Acta*, 2012, **82**, 397–401.
4 T. Abe, K. Fukui, Y. Kawai, K. Nagai and H. Kato, *Chem. Commun.*, 2016, **52**, 7735–7737.
5 K. Tsuji, O. Tomita, M. Higashi and R. Abe, *ChemSusChem*, 2016, **9**, 2201–2208.
6 T. Grewe and H. Tüysüz, *J. Mater. Chem. A*, 2016, **4**, 3007–3017.
7 J. Yan, H. Wu, H. Chen, Y. Zhang, F. Zhang and S. Liu, *Appl. Catal., B*, 2016, **190**, 130–137.
8 R. Kobayashi, T. Takashima, S. Tanigawa, S. Takeuchi, B. Ohtani and H. Irie, *Phys. Chem. Chem. Phys.*, 2016, **18**, 27754–27760.
9 Q. Wang, T. Hisatomi, Q. Jia, H. Tokudome, M. Zhong, C. Wang, Z. Pan, T. Takata, M. Nakabayashi, N. Shibata, Y. Li, I. Sharp, A. Kudo, T. Yamada and K. Domen, *Nat. Mater.*, 2016, **15**, 611–615.
10 J. Zhang, H. Ma and Z. Liu, *Appl. Catal., B*, 2017, **201**, 84–91.
11 C. Fàbrega, S. Murcia-López, D. Monllor-Satoca, J. D. Prades, M. D. Hernández-Alonso, G. Penelas, J. R. Morante and T. Andreu, *Appl. Catal., B*, 2016, **189**, 133–140.
12 X. Shi, I. Herraiz-Cardona, L. Bertoluzzi and P. Lopez-Varo, *Phys. Chem. Chem. Phys.*, 2016, **18**, 9255–9261.
13 J. Zhao, E. Olide and F. E. Osterloh, *J. Electrochem. Soc.*, 2015, **162**, H65–H71.
14 D. Chandra, K. Saito, T. Yui and M. Yagi, *Angew. Chem., Int. Ed.*, 2013, **52**, 12606–12609.
15 A. Kleiman-Shwarsctein, A. B. Laursen, F. Cavalca, W. Tang, S. Dahla and I. Chorkendorff, *Chem. Commun.*, 2012, **48**, 967–969.
16 R. Liu, Y. Lin, L.-Y. Chou, S. W. Sheehan, W. He, F. Zhang, H. J. M. Hou and D. Wang, *Angew. Chem., Int. Ed.*, 2011, **50**, 499–502.
17 C. Santato, M. Ulmann and J. Augustynski, *J. Phys. Chem. B*, 2001, **105**, 936–940.
18 B. D. Alexander, P. J. Kulesza, I. Rutkowska, R. Solarskac and J. Augustynski, *J. Mater. Chem.*, 2008, **18**, 2298–2303.
19 S. Sfaelou, L.-C. Pop, O. Monfort, V. Dracopoulos and P. Lianos, *Int. J. Hydrogen Energy*, 2016, **41**, 5902–5907.
20 K. Maeda and K. Domen, *J. Phys. Chem. C*, 2007, **111**, 7851–7861.
21 T. Jin, P. Diao, Q. Wu, D. Xu, D. Hu, Y. Xie and M. Zhang, *Appl. Catal., B*, 2014, **148–149**, 304–310.
22 Q. Mi, A. Zhanaidarova, B. S. Brunschwig, H. B. Gray and N. S. Lewis, *Energy Environ. Sci.*, 2012, **5**, 5694–5700.
23 D. Monllor-Satoca, L. Borja, A. Rodes, R. Gómez and P. Salvador, *ChemPhysChem*, 2006, **12**, 2540–2551.

24 A. Fujishima and K. Honda, *Nature*, 1972, **238**, 37–38.

25 L. N. Quan, Y. H. Jang, K. A. Stoerzinger, K. J. May, Y. J. Jang, S. T. Kochuveedu, Y. Shao-Horn and D. H. Kim, *Phys. Chem. Chem. Phys.*, 2014, **16**, 9023–9030.

26 H. Li, J. Chen, Z. Xia and J. Xing, *J. Mater. Chem. A*, 2015, **3**, 699–705.

27 S. Hernández, D. Hidalgo, A. Sacco, A. Chiodoni, A. Lamberti, V. Cauda, E. Tresso and G. Saracco, *Phys. Chem. Chem. Phys.*, 2015, **17**, 7775–7786.

28 M. S. Wrighton, D. S. Ginley, P. T. Wolczanski, A. B. Ellis, D. L. Morse and A. Linz, *Proc. Natl. Acad. Sci. U. S. A.*, 1975, **72**, 1518–1522.

29 A. Fujishima, K. Kohayakawa and K. Honda, *J. Electrochem. Soc.*, 1975, **122**, 1487–1489.

30 T. Abe, K. Nagai, S. Kabutomori, M. Kaneko, A. Tajiri and T. Norimatsu, *Angew. Chem., Int. Ed.*, 2006, **45**, 2778–2781.

31 K. Nagai, T. Abe, Y. Kaneyasu, Y. Yasuda, I. Kimishima, T. Iyoda and H. Imaya, *ChemSusChem*, 2011, **4**, 727–730.

32 K. Nagai, Y. Yasuda, T. Iyoda and T. Abe, *ACS Sustainable Chem. Eng.*, 2013, **1**, 1033–1039.

33 T. Abe, M. Okumura, Y. Kikuchi, T. Itoh and K. Nagai, *J. Mater. Chem. A*, 2017, **5**, 7445–7450.

34 P. Arunachalam, S. Zhang, T. Abe, M. Komura, T. Iyoda and K. Nagai, *Appl. Catal., B*, 2016, **193**, 240–247.

35 D. Mendori, T. Hiroya, M. Ueda, M. Sanyoushi, K. Nagai and T. Abe, *Appl. Catal., B*, 2017, **205**, 514–518.

36 T. Abe, N. Taira, Y. Tanno, Y. Kikuchi and K. Nagai, *Chem. Commun.*, 2014, **50**, 1950–1952.

37 T. Abe, Y. Tanno, N. Taira and K. Nagai, *RSC Adv.*, 2015, **5**, 46325–46329.

38 T. Abe, K. Nagai, K. Sekimoto, A. Tajiri and T. Norimatsu, *Electrochem. Commun.*, 2005, **7**, 1129–1132.

39 T. Abe, S. Tobinai, N. Taira, J. Chiba, T. Itoh and K. Nagai, *J. Phys. Chem. C*, 2011, **115**, 7701–7705.

40 T. Abe, Y. Hiyama, K. Fukui, K. Sahashi and K. Nagai, *Int. J. Hydrogen Energy*, 2015, **40**, 9165–9170.

41 R. Saito, H. Ueno, J. Nemoto, Y. Fujii, A. Izuoka and M. Kaneko, *Chem. Commun.*, 2009, **2009**, 3231–3233.

42 F. Amano, E. Ishinaga and A. Yamakata, *J. Phys. Chem. C*, 2013, **117**, 22584–22590.

43 T. Jin, P. Diao, D. Xu and Q. Wu, *Electrochim. Acta*, 2013, **114**, 271–277.

44 W. Zhao, Z. Wang, X. Shen, J. Li, C. Xu and Z. Gan, *Int. J. Hydrogen Energy*, 2012, **37**, 908–915.

45 Y. Hou, F. Zuo, A. P. Dagg, J. Liu and P. Feng, *Adv. Mater.*, 2014, **26**, 5043–5049.

46 I. Fujimoto, N. Wang, R. Saito, Y. Miseki, T. Gunji and K. Sayama, *Int. J. Hydrogen Energy*, 2014, **39**, 2454–2461.

47 J. Akikusa and S. U. M. Khan, *Int. J. Hydrogen Energy*, 2002, **27**, 863–870.

48 M. Radecka, M. Rekas, A. Trenczek-Zajac and K. Zakrzewska, *J. Power Sources*, 2008, **181**, 46–55.

49 M. Moriya, T. Minegishi, H. Kumagai, M. Katayama, J. Kubota and K. Domen, *J. Am. Chem. Soc.*, 2013, **135**, 3733–3735.

50 R. Abe, M. Higashi and K. Domen, *ChemSusChem*, 2011, **4**, 228–237.

51 K. Maeda, M. Higashi, D. Lu, R. Abe and K. Domen, *J. Am. Chem. Soc.*, 2010, **132**, 5858–5868.

52 H. Kato, Y. Sasaki, N. Shirakura and A. Kudo, *J. Mater. Chem. A*, 2013, **1**, 12327–12333.